Organic Electronics 15 (2014) 111–117

Contents lists available at ScienceDirect

Organic Electronics

journal homepage: www.elsevier.com/locate/orgel

Highly improved light extraction with a reduced spectrum distortion of organic light-emitting diodes composed by the sub-visible wavelength nano-scale periodic (~250 nm) structure and micro-lens array

Kyung Bok Choi [a], Se Joong Shin [b], Tae Hyun Park [a], Hyun Jun Lee [a], Ju Hyun Hwang [a], Jung Ho Park [b], Bo Yeon Hwang [a], Young Wook Park [c,1], Byeong-Kwon Ju [a,*]

[a] Display and Nanosystem Laboratory, College of Engineering, Korea University, Seoul 136-713, Republic of Korea
[b] Samsung Display Co., Ltd., Tangjeong-Myeon, Asan-City, Chungcheongnam-Do, Republic of Korea
[c] The Institute of High Technology Materials and Devices, Korea University, Seoul 136-713, Republic of Korea

ARTICLE INFO

Article history:
Received 2 September 2013
Received in revised form 18 October 2013
Accepted 20 October 2013
Available online 6 November 2013

Keywords:
Laser interference lithography (LIL)
Organic light-emitting diodes (OLEDs)
Nano-scale periodic pattern
Out-coupling
Micro-lens arrays
Photonic crystal

ABSTRACT

Out-coupling enhanced organic light-emitting diodes (OLEDs) with micro-lens arrays and a nano-scale periodic light-extraction structure—a photonic crystal (PC)—utilizing laser interference lithography (LIL) are demonstrated. Generally, PC-based OLEDs suffer from a distorted and shifted spectrum, despite a highly improved intensity. However, in this study, we demonstrate PC-based OLEDs with a distortion-free spectrum and a highly improved out-coupling performance. It was found that spectrum distortion decreased with the pitch size of the PC. The PC-based OLED with a 250 nm pitch size showed a dramatically reduced spectral shift: International Commission on Illumination 1931 color coordinate of (Δ0.00, Δ0.00) and Δpeak wavelength of 0 nm as compared with the reference. Simultaneously, the external quantum efficiency and the power efficiency were enhanced by up to 178% and 264%, respectively, as compared with the reference. Moreover, through the LIL, simple and maskless processes were achieved for a light-extraction structure over a large area.

1. Introduction

Recently, organic light-emitting diodes (OLEDs) have been studied for outstanding display [1] and solid-state lighting [2] owing to their low power consumption, fast response time, excellent color reproduction, and good physical features such as low thickness, lightness, flexibility, and transparency. Despite the rapid development of OLEDs, problems remain. Although it has been reported that almost 100% internal quantum efficiency (η_{IQE}) was theoretically achieved [3], many issues on the light out-coupling efficiency (η_{out}) of 20% at most have remained. This phenomenon is generated by the waveguide effect and the total internal reflection attributed to the difference in the refractive indexes among the organic materials ($n_{org} \approx 1.7$), indium tin oxide (ITO) ($n_{ITO} \approx 1.8$), glass substrate ($n_{substrate} \approx 1.5$), and air ($n_{air} \approx 1$) [4]. Due to this low η_{out}, it is need to increase operation voltage and current density that make the degradation of OLEDs device became much faster.

To overcome this issue, various approaches to enhance the out-coupling of the OLEDs have become a major topic in OLED research. These studies are divided into two themes. Studies on the light extraction from the substrate to the air, including a micro-lens array (MLA) [5–8], brightness-enhancement film [9], high refractive index substrate [10], and scattering layer [11], have been reported. The

* Corresponding author. Tel.: +82 2 3290 3237; fax: +82 2 3290 3791.
E-mail addresses: zerook@korea.ac.kr (Y.W. Park), bkju@korea.ac.kr (B.-K. Ju).
[1] Co-corresponding author.

1566-1199/$ - see front matter © 2013 Elsevier B.V. All rights reserved.
http://dx.doi.org/10.1016/j.orgel.2013.10.021

out-coupling enhancement that occurs in the stack of materials above the substrate has also been studied, which contained a low-index grid [12], aperiodic dielectric mirrors [13], buckle structure [14], photonic crystal (PC) structures [15,16], an aerogel layer [17], and a patterned ITO [18]. Nevertheless, these methods sometimes suffer from disadvantages such as complex and very expensive fabrication process, low yield or limited enhancement [19], angular dependence [13], and distorted and shifted spectra [16,20]. In particular, the out-coupling enhancement technique that uses the PC structure has been reported as an effective method owing to its simple and highly improved intensity even top OLEDs using the resonance of emission wave [15,16,25]; however, the PC-structure OLEDs generally have a strong distorted spectrum [16,20,21], which limits their application as light sources and in displays. Thus far, PC structures for light extraction have been mostly fabricated by techniques such as nano-imprint lithography [22] and electron-beam lithography [23]. These methods involve high costs and are not suitable for large-area fabrication.

In this study, we demonstrate high-efficiency distortion-free spectrum OLEDs using PC and MLA. The PC structure is fabricated by laser interference lithography (LIL), which enables simple and cost-intensive manufacturing for a maskless and largely scalable process. We obtain a very significant result using a 250 nm pitch size PC-based OLED with MLA. As compared with the reference, the external quantum efficiency (EQE) improves by 178%. Moreover, in spite of the PC-based OLEDs, it shows distortion-free performance in the International Commission on Illumination (CIE) 1931 color coordinate as (Δ0.00, Δ0.00) and a 0 nm Δpeak wavelength shift from the reference.

2. Experiment

Fig. 1 shows the entire OLEDs fabrication process. To fabricate the patterned substrate, first, the 500 nm-thick SiO_2 deposited Eagle XG glass (Corning, Inc.) was cleaned in an ultrasonic bath with acetone, methanol, and deionized water and dried in an oven. For better adhesion of the photoresist (PR), hexamethyldisilazane (HMDS) was spin coated on the SiO_2 surface, and the PR (AR-N 4240:AR 300-12 = 1:1, Allresist Co., Ltd.) was subsequently spin coated for 40 s at 4000 rpm and annealed on a hot plate for soft baking. LIL was performed on the samples using a Lloyd's mirror interferometer, under air atmosphere schematically shown in Fig. 2.

The laser is a frequency-doubled Ar-ion laser with a wavelength of 257 nm and a power of 0.14 mW/cm^2, measured by an optical power energy meter (1936-C, Newport Co., Ltd.). To create the PR hole patterns, the samples were exposed twice with a 90° rotation for 85 s, annealed on a hot plate for post baking, and developed using an exclusive developer (AR 300-47, Allresist Co., Ltd.). The periodicity, i.e., P of the PR pattern (called the pitch size) was determined by

$$P = \frac{\lambda}{2\sin\theta} \tag{1}$$

where λ is the wavelength of the laser, and θ is the incident angle of the laser beam with the sample [24]. By changing the value of θ from 13° to 30°, pitch size control from 550 nm to 250 nm was achieved. Next, the SiO_2 was dry etched using CF_4 plasma by reactive ion etching, using the patterned PR as an etching mask. Then, the PR was removed using an exclusive PR remover and O_2 plasma treatment. The nano-patterned substrates showed slightly decreased transmittance (−5 to 0% at visible wavelength) than Eagle XG glass.

In the second step, radio-frequency sputter was used to deposit the ITO transparent anode with a thickness of 200 nm and a sheet resistance of 35 Ω/sq. Then, the MLA (prototype MLA sheet, MNtech. Co., Ltd.) was attached to the glass side of the substrate opposite the ITO. The OLEDs, with an active area of 4 × 4 mm, were fabricated by a thermal evaporator in high vacuum (~2×10^{-6} Torr). And the devices were consisted of 60 nm of N,N′-bis(naphthalene-1-yl)-N,N′-bis(phenyl)-benzidine as the hole transport layer, 80 nm of tris(8-hydroxy-quinolinato) aluminum as the emission layer, 0.8 nm-thick lithium fluoride as the electron injection layer, and 100 nm-thick aluminum as the cathode. The deposition rates of all organic materials and metals were ~1 Å/s and ~5 Å/s, respectively. To

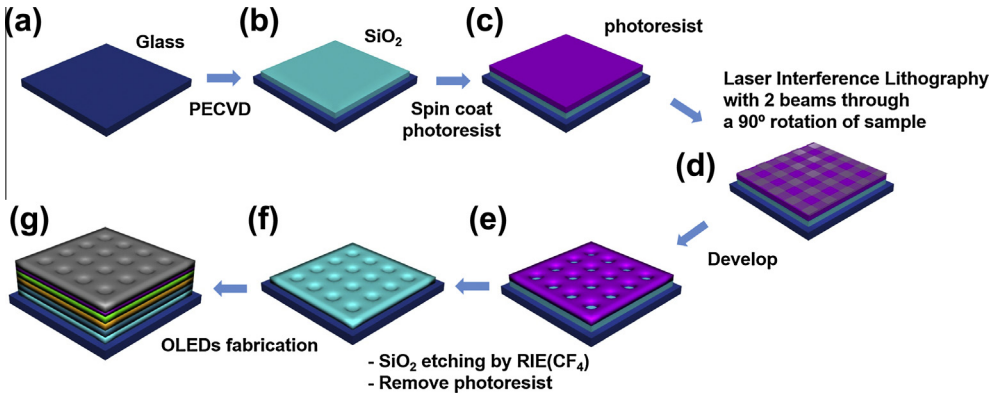

Fig. 1. Schematic diagram of the fabrication process of OLEDs with nano-scale pattern. Through LIL, the nano-pattern is created. Over the nano-pattern on the substrate, the OLEDs are manufactured by thermal evaporation.

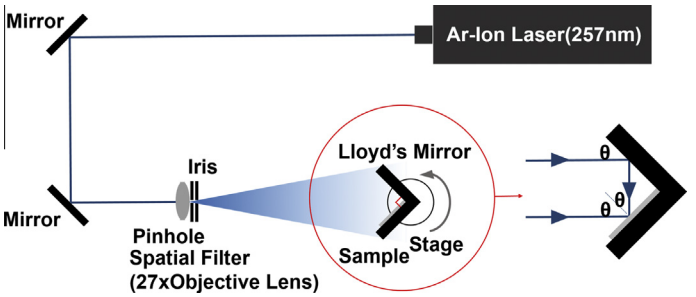

Fig. 2. Illustration of the LIL system. The laser is a frequency-doubled Ar-ion laser with a 257 nm wavelength. To create the hole pattern, two exposures by rotating the specimen by 90° in between are applied.

compare the performance of the OLEDs, we fabricated 12 types of devices through a three-batch process according to the pitch size, namely, non-nano-patterned devices without and with MLA and nano-patterned devices without and with MLA on the pitch. As conventional and reference devices, Ref.-1, Ref-2, and Ref.-3 were fabricated without nano-patterns. Ref.-1 + MLA, Ref.-2 + MLA, and Ref.-3 + MLA were fabricated without nano-patterns but with MLA. For Device-1, Device-2, and Device-3, the substrate pattern sizes were 550, 350, and 250 nm, respectively. For Device-1 + MLA, Device-2 + MLA, and Device-3 + MLA, the pattern sizes of the devices were respectively similar to the previous devices, and MLA was attached at the same time. The structures of the OLEDs are shown in Fig. 3, where (a) shows the non-nano-patterned devices and (b) shows the nano-patterned devices with MLA, which have a corrugated structure with periodic SiO_2 pattern.

Finally, the electroluminescence (EL) characteristics of the fabricated OLEDs were measured using a spectroradiometer (PR-670 SpectraScan, Photo Research, Inc.) and a high-voltage source measurement unit (Model 237, Keithley Instruments, Inc.) in a dark box without any passivation layer under an air condition and at room temperature.

3. Results and discussion

Fig. 3c shows the electrical characteristics of the device and reference. As corrugated structure by PC-structure seen Fig. 3b, the plot of current density as a function of the voltage shows decreased the operation voltage [14]. In addition, nano-patterned device shows good performance more than reference for light extraction. At the same time, any decrease or changes about luminance and current density did not found during the operation.

Fig. 4 shows the scanning electron microscope (SEM) images of the 550, 350 and 250 nm patterned substrate. The inset in Fig. 4 shows the photographic image of the nano-patterned 2.5 cm × 2.5 cm glass substrate. As mentioned earlier, the PC-based OLEDs suffer from a distorted spectrum [20,21]. The inset in Fig. 4 shows the distortion of the light through the rainbow effect at the sample surface. Nevertheless, when the pitch size was decreased to 250 nm, the rainbow effect can be barely seen, which means that using a pitch size of less than half the emissive wavelength, PC-based OLEDs with reduced spectrum distortion can be fabricated [17].

Fig. 5 shows the EL spectra of the fabricated PC-based OLEDs. Table 1 shows the summarized spectral analysis. Fig. 5a shows the EL spectra of the PC-based OLED with a 550 nm pitch size. Device-1 and Device-1 + MLA show lesser distortion spectrum: Δpeak wavelength = −2 nm and ΔCIE′ 1931 = (0.00, +0.01), Δpeak wavelength = −8 nm and ΔCIE′ 1931 = (−0.01, 0.00). In the 550-nm pitch-size PC OLED, the spectrum distortion is relatively low. Due to the low PC effect by the wide pitch oriented much smoother surface during isotropic RIE process of the 550 nm pitch-size PC OLEDs, the 550 nm pitch-size PC OLED shows relatively low spectrum distortion. Fig. 5b shows the EL spectra of the PC-based OLED with a 350 nm pitch size.

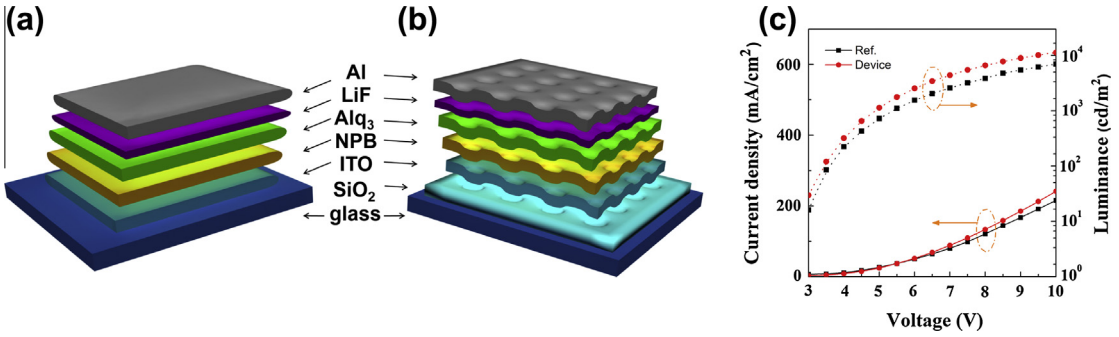

Fig. 3. Schematic of the OLED structure. (a) Reference; (b) PC-based OLED with nano-pattern by the LIL. Because of the nano-scale periodic structure, the structure appears to be wrinkled and (c) current density and luminance as a function of voltage for reference and PC-based OLEDs.

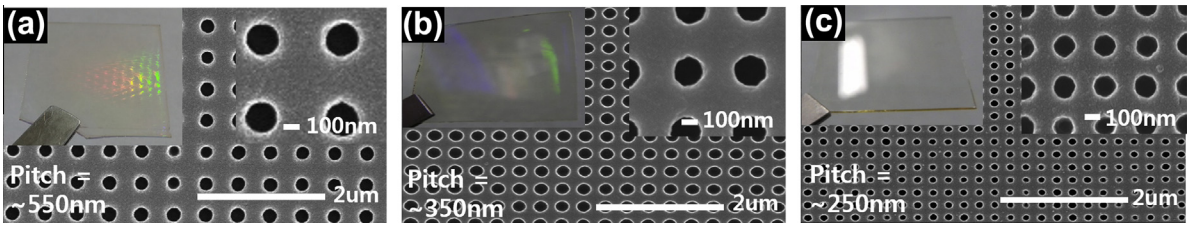

Fig. 4. SEM images according to the pitch size with different θs. The inset shows the optical image of the sample. (a) Approximately 550 nm pitch size sample; (b) Approximately 350 nm pitch size sample; and (c) Approximately 250 nm pitch size sample.

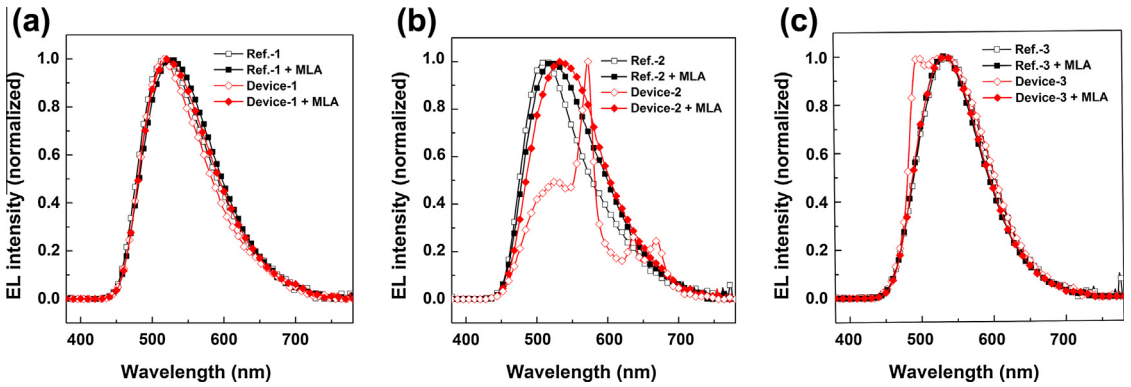

Fig. 5. Spectrum analysis of the devices. Normalized EL intensity as a function of the wavelength: (a) Devices with 550 nm pitch size structure OLEDs and the reference; (b) Devices with 350 nm pitch size structure OLEDs and the reference; and (c) Devices with 250 nm pitch size structure OLEDs and the reference. The open symbol shows the devices without MLA, and the solid symbol shows the devices with MLA.

Table 1
Spectrum and CIE′ color coordinates of the nano-patterned devices and references.

MLA	Device	550 nm pitch size		350 nm pitch size		250 nm pitch size	
		Max (nm)	CIE′ 1931	Max (nm)	CIE′ 1931	Max (nm)	CIE′ 1931
Without MLA	Ref.	518	(0.32, 0.52)	512	(0.31, 0.51)	538	(0.35, 0.55)
	Device	516	(0.32, 0.53)	572	(0.37, 0.53)	532	(0.34, 0.54)
		Δ = −2	(Δ0.00, +Δ0.01)	Δ = +60	(+Δ0.06 +Δ0.02)	Δ = −6	(−Δ0.01, −Δ0.01)
With MLA	Ref. + MLA	528	(0.34, 0.53)	520	(0.34, 0.52)	532	(0.34, 0.55)
	Device + MLA	520	(0.33, 0.53)	532	(0.36, 0.53)	532	(0.34, 0.55)
		Δ = −8	(−Δ0.01, Δ0.00)	Δ = +12	(+Δ0.02, +Δ0.01)	Δ = 0	(Δ0.00, Δ0.00)

The Device-2 spectrum was too distorted to reflect the shape of Ref.-2: Δpeak wavelength = +60 nm and ΔCIE′ 1931 = (+0.06, +0.02). However, the Device-2 + MLA spectrum was considerably restored: Δpeak wavelength = +12 nm and ΔCIE′ 1931 = (+0.02, +0.01). The MLA works as a light extraction layer for the trapped light in the substrate mode by refractive index matching, and the hemispheric shape induces high out-coupling of the MLA/air interface, reducing the distortion. On the other hand, Fig. 5c shows that Device-3 has much reduced spectrum shift and distortion except at around 500 nm: Δpeak wavelength = −6 nm and ΔCIE′ 1931 = (−0.01, −0.01). Device-3 + MLA shows an almost similar spectrum with the reference. As compared with Device-2, the difference in the distortion can be easily observed. The distortion decreases evidently. Moreover, when the MLA is attached to the OLED (Device-3 + MLA), the spectrum almost matches that of the reference (Δpeak wavelength = 0 nm and ΔCIE′ 1931 = (0.00, 0.00), which is negligible). Thus, it indicates more enhanced performance than the samples with different pitch sizes. As the pitch size is reduced, the spectral distortion is reduced, followed by EL efficiency enhancement. Further improvement is expected with the reduction in the pitch size of the PC structure and the optimized pitch depth. This pitch-size-dependent property of the spectral distortion and EL performance indicates the possibility of realizing high-efficiency OLEDs lightings using a high-throughput nano-scale structure fabrication process. Fig. 6 shows the spectra on the angle dependent measurement regarding reference and 250 nm pitch-size device. The measurement was conducted from 0° to the 60° interval with 15° without MLA. In the case of reference, the

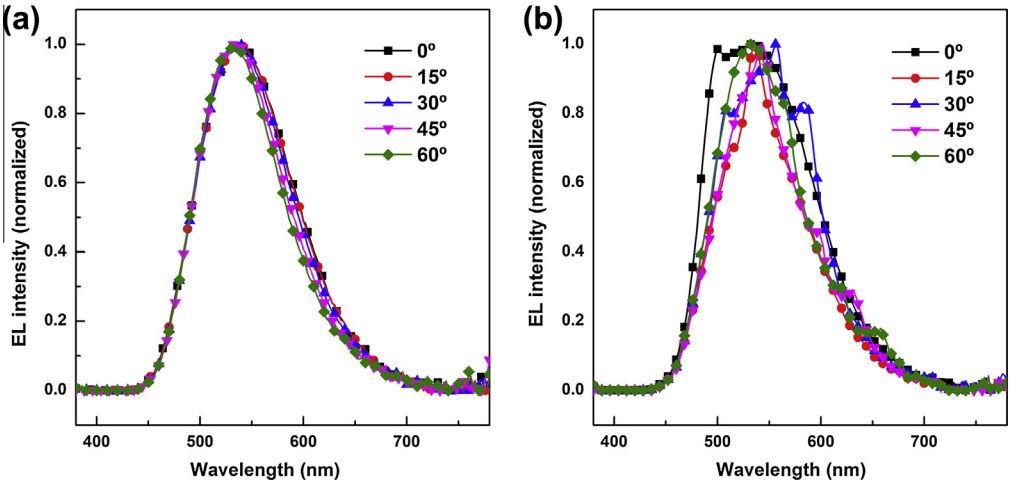

Fig. 6. (a) EL intensity of reference as a function of the wavelength. (b) EL intensity of 250 nm pitch-size device as a function of the wavelength. Both are measured at angles of 0°, 15°, 30°, 45°, 60° without MLA.

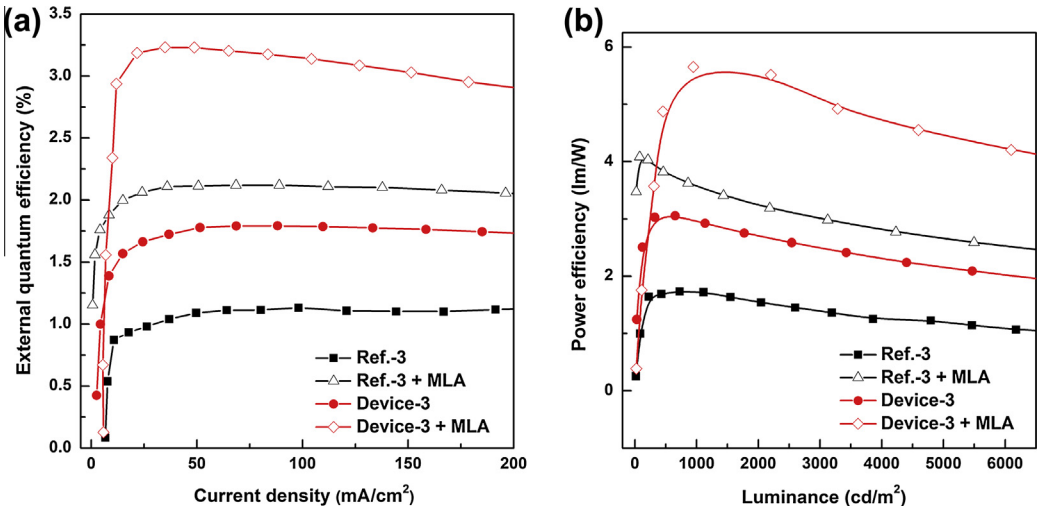

Fig. 7. (a) EQE as a function of the current density of the nano-patterned device with a pitch size of 250 nm and references. (b) PE as a function of the luminance. In both (a) and (b), the solid symbols represent the performance of the devices without MLA, and the open symbols indicate the performance of the devices with MLA.

shape was relatively regular but in the case of device, it shows the spectrum variation as the viewing angle as other PC-based OLEDs. Nonetheless, measurement at 0° with MLA shows distortion free spectrum distribution seen Fig. 5c.

The performances of the devices with a pitch size of 250 nm which spectrum are similar with reference are shown in Fig. 7, which consists of the devices with and without the MLA.

Table 2 presents the summary of the device performance. Although the nano-patterned devices shows much wider light distribution than Lambertian profile, due to limited measurement conditions the presented values were calculated assuming Lambertian emission. Fig. 7a shows the EQE as a function of the current density. The EQEs are 1.13% (Ref.-3) and 1.79% (Device-3) for the devices with no MLA whereas those with the MLA are 2.11% Ref.-3 + MLA and 3.15% (Device-3 + MLA) at 100 mA/cm^2. The out-coupling process divided into two steps of the increasing the glass mode by nano-patterned substrate and the extracting the glass mode light into air mode by MLA. The Device-3 (nano-patterned substrate) shows 58% enhancement of EQE than that of Ref.-3. That means the glass and air mode are increased by the diffraction on the nano-pattern. However, in the case of Ref.-3 + MLA, device only applied MLA, it recorded 86% enhancement. We assumed that the prototype MLA (hemisphere height is ~50 μm, diameter is ~70 μm and MLA total thickness is 0.33 mm) by MNtech Co., Ltd. play an important role to record high improvement. The Device-3 + MLA shows the best performance. The EQE was enhanced by 178% as compared with that of Ref.-3 and was increased

Table 2
Performance of the 250 nm pitch size patterned OLEDs and the references.

Device	EQE (%) at 100 m A/cm	EQE improvement factor		PE (Im/W) at 3000 cd/m^2	PE improvement factor	
		Compared to Ref.-3 (%)	Compared to Ref.-3 + MLA (%)		Compared to Ref.-3 (%)	Compared to Ref.-3 + MLA (%)
Ref.-3	1.13	–	–	1.39	–	–
Device-3	1.79	+58	–	2.49	+79	–
Ref.-3 + MLA	2.11	+86	–	3.01	+116	–
Device-3 + MLA	3.15	+178	+49%	5.07	+264	+68

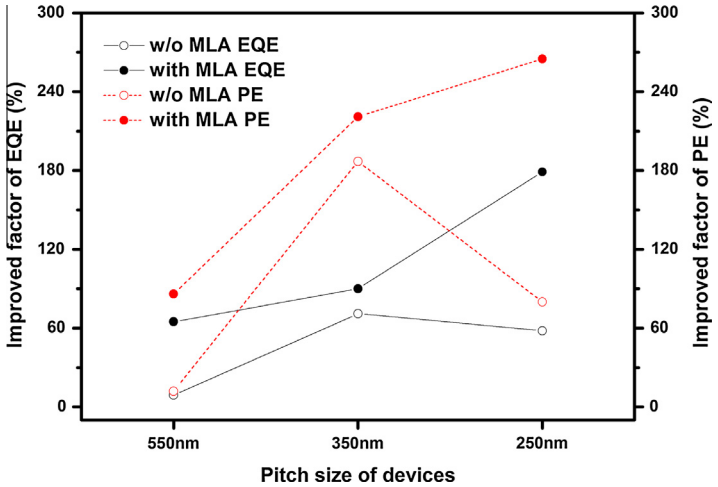

Fig. 8. Improvement factor of the device by changing the pitch size from 550 nm to 250 nm as compared with the reference with no PC structure and MLA.

by 49% as compared with that of the Ref.-3 + MLA. The results show that, using MLA, the EQEs of all devices are enhanced as compared with that of the device with only a nanostructure. In addition, comparing the effect of applying MLA, since the light in the air mode was already extracted by nano-pattern in the Device-3 + MLA, the improvement factor of 49% were relatively lower than that of Ref.-3 + MLA (86%). Fig. 7b shows the power efficiency (PE) as a function of luminance. The PEs at a luminance of 3000 cd/m^2 are 1.39 lm/W (Ref.-3), 2.49 lm/W (Device-3), 3.01 lm/W (Ref.-3 + MLA), and 5.07 lm/W (Device-3 + MLA). Device-3 + MLA shows the best performance of 5.07 lm/W—an improvement of 264% as compared with that of Ref.-3. Meanwhile, over 100% enhancement of Ref.-3 + MLA is just not from the MLA, the corrugated nano-structure also effects an improvement of the PE. Because the structure decreased the operation voltage of the device, the PE could be enhanced.

In terms of the pitch size, the enhanced efficiency is different.

Fig. 8 shows the improvement factor as compared with the reference (non-nano-patterned) in terms of the pitch size. In the OLEDs with no MLA, at a 550 nm pitch size, the device shows less distorted spectrum but shows the lowest improvement factor of EQE and PE. This is interpreted as the less corrugated structure as compared with that of the low-pitch-size sample, similarity between the pitch size and the wavelength of the extracted light, and as decreased air-mode light. In the devices with MLA, the EQEs of all devices are enhanced as compared with those with no MLA. This phenomenon shows that the MLA extracted the glass mode light increased by the PC structure. In particular, the 250 nm-pitch PC-based OLED shows the most enhanced performance at 178%. In the case of the PE, the plot for the devices with MLA shows enhanced performance as compared with that without MLA. For the 350 and 250 nm pitch-size devices with MLA, the improvement factor surged over 200%.

These results indicate that the nano-scale pattern plays an important role in increasing the out-coupling efficiency and reducing the distortion. Owing to this structure, the light path can be changed, possibly reducing the non-emissive waveguide mode; thus, light can be out-coupled outside the substrate. Moreover, we confirm that the device with low pitch size shows a distortion-free spectrum. When the MLA is attached, the efficiency increases because of the extraction of the light trapped in the PC structure substrate by refractive index matching and because of the out-coupling of light to the air owing to the hemispheric shape. In addition, by using the MLA, the spectrum distortion is minimized. These results indicate that low pitch-size PC-based OLEDs can be fabricated as corrugated-structure OLEDs with a distortion-free spectrum and high efficiency.

4. Conclusions

In conclusion, by using a PC structure with a pitch size smaller than half of the emissive wavelength, we have demonstrated the high efficiency spectral distortion-free OLEDs using LIL-processed PC and MLA. Unlike the conventional method of fabricating periodic patterns, such as the E-beam lithography and imprinting, with the simple LIL process, the fabrication cost was lower. At the same time, the patterning process was maskless and suitable for large-scale fabrication. According to the pitch size, we found that the efficiency improvement and spectrum distortion were different. The corrugated structure of the OLEDs, the PC structure of the substrate, and the MLA affected these characteristics. In particular, the demonstrated performance of the devices with a 250 nm pitch size PC and MLA showed a distortion-free spectrum and more enhanced characteristics than the PC-based OLEDs with different sizes, achieving an EQE of up to 178% and a PE of 264%. Thus, we have developed a technology for efficiency-enhanced OLEDs (which overcome the disadvantage of the PC structure), which required low cost and a large-area process using the enhanced OLEDs as lighting sources. Also the effect of the ratio between hole and fixed pitch size, the influence of the under 250 nm pitch size pattern on efficiency and applications for top OLEDs are to be studied as a future research.

Acknowledgments

K.B Choi and S.J Shin contributed equally to this work. This research was supported by the Basic Science Research Program through the National Research Foundation of Korea (NRF) funded by Korea government (MSIP) (CAFDC/Byeong-Kwon Ju/No. 2007-0056090), the NRF Project of the MEST (No. 2012R1A6A3A04039396), and the IT R&D Program of MKE/KEIT (No. 2009-F-016-01, Development of Eco-Emotional OLED Flat-Panel Lighting). The authors thank the staff of KBSI for technical assistance.

References

[1] P.E. Burrows, G. Gu, V. Bulović, Z. Shen, S.R. Forrest, M.E. Thompson, IEEE Trans. Electron Devices 44 (1997) 1188.
[2] S. Reineke, F. Lindner, G. Schwartz, N. Seidler, K. Walzer, B. Lüssem, K. Leo, Nature 459 (2009) 234.
[3] C. Adachi, M.A. Baldo, M.E. Thompson, S.R. Forrest, J. Appl. Phys. 90 (2001) 5048.
[4] G. Gu, D.Z. Garbuzov, P.E. Burrows, S. Venkatesh, S.R. Forrest, M.E. Thompson, Opt. Lett. 22 (1997) 396.
[5] S. Möller, S.R. Forrest, J. Appl. Phys. 91 (2002) 3324.
[6] M.K. Wei, I.L. Su, Opt. Express 12 (2004) 5777.
[7] Y. Sun, S.R. Forrest, J. Appl. Phys. 100 (2006) 073106.
[8] S.H. Eom, E. Wrzesniewski, J. Xue, Org. Electron. 12 (2011) 472.
[9] H.Y. Lin, J.H. Lee, M.K. Wei, C.L. Dai, C.F. Wu, Y.H. Ho, H.Y. Lin, T.C. Wu, Opt. Commun. 275 (2007) 464.
[10] S. Mladenovski, K. Neyts, D. Pavicic, A. Werner, C. Othe, Opt. Express 17 (2009) 7562.
[11] R. Bathelt, D. Buchhauser, C. Gärditz, R. Paetzold, P. Wellmann, Org. Electron. 8 (2007) 293.
[12] Y. Sun, S.R. Forrest, Nat. Photon. 2 (2008) 483.
[13] M. Agrawal, Y. Sun, S.R. Forrest, P. Peumans, Appl. Phys. Lett. 90 (2007) 241112.
[14] W.H. Koo, S.M. Jeong, F. Araoka, K. Ishikawa, S. Nishimura, T. Toyooka, H. Takezoe, Nat. Photon. 4 (2010) 222.
[15] M. Fujita, T. Ueno, K. Ishihara, T. Asano, S. Noda, H. Ohata, T. Tsuji, H. Nakada, N. Shimoji, Appl. Phys. Lett. 85 (2004) 5769.
[16] A.O. Altun, S. Jeon, J. Shim, J.H. Jeong, D.G. Choi, K.D. Kim, J.H. Choi, S.W. Lee, E.S. Lee, H.D. Park, J.R. Youn, J.J. Kim, Y.H. Lee, J.W. Kang, Org. Electron. 11 (2010) 711.
[17] T. Tsutsui, M. Yahiro, H. Yokogawa, K. Kawano, M. Yokoyama, Adv. Mater. 13 (2001) 1149.
[18] T.W. Koh, J.M. Choi, S. Lee, S. Yoo, Adv. Mater. 22 (2010) 1849.
[19] T. Nakamura, N. Tsutsumi, N. Juni, H. Fujii, J. Appl. Phys. 97 (2005) 054505.
[20] D.K. Gifford, D.G. Hall, Appl. Phys. Lett. 81 (2002) 4315.
[21] Y.R. Do, Y.C. Kim, Y.W. Song, C.O. Cho, H. Jeon, Y.J. Lee, S.H. Kim, Y.H. Lee, Adv. Mater. 15 (2003) 1214.
[22] K. Ishihara, M. Fujita, I. Matsubara, T. Asano, S. Noda, H. Ohata, A. Hirasawa, H. Nakada, N. Shimoji, Appl. Phys. Lett. 90 (2007) 111174.
[23] M. Fujita, K. Ishihara, T. Ueno, T. Asano, S. Noda, H. Ohata, T. Tsuji, H. Nakada, N. Shimoji, Jpn. J. Appl. Phys. 44 (2005) 3669.
[24] M. Walsh, On the design of lithographic interferometers and their applications, Ph.D. thesis, MIT, September 2004.
[25] Y. Jin, J. Feng, X.L. Zhang, Y.G. Bi, Y. Bai, L. Chen, T. Lan, Y.F. Liu, Q.D. Chen, H.B. Sun, Adv. Mater. 24 (2012) 1187.